

Stability and hybridization-driven aggregation of silver nanoparticle–oligonucleotide conjugates

Bernardo C. Vidal Jr.,^a Theivanayagam C. Deivaraj,^a Jun Yang,^b Heng-Phon Too,^{ac} Gan-Moog Chow,^{ad} Leong M. Gan^e and Jim Y. Lee^{*abe}

^a Singapore-MIT Alliance, National University of Singapore, Singapore.

E-mail: cheleejy@nus.edu.sg; Fax: +65 67791936; Tel: +65 68742899

^b Department of Chemical and Biomolecular Engineering, National University of Singapore, 10 Kent Ridge Crescent Singapore 1190260

^c Department of Biochemistry, National University of Singapore, Singapore

^d Department of Materials Science, National University of Singapore, Singapore

^e Institute of Materials Research and Engineering, Agency for Science, Technology and Research (A*Star), Singapore

Received (in Montpellier, France) 22nd November 2004, Accepted 18th March 2005

First published as an Advance Article on the web 25th April 2005

Gold nanoparticles are well known to form stable oligonucleotide conjugates, *via* thiol–metal interaction, which are capable of specific DNA-hybridization induced aggregation. Preparation of an analogous conjugate with Ag particles, except when coated with a layer of Au, has been reported to yield conjugates that are unstable in the hybridization environment. We report herein the hybridization-induced aggregation of such “bare” Ag-particle conjugates prepared *via* a similar facile procedure to Au with slight modification. We found that the pH during functionalization is the critical factor determining the success of preparing conjugates that remain stable throughout the functionalization process and during hybridization. We reasoned that this is a consequence of the pH-dependent charge of the oligonucleotide, and demonstrated that pH strongly affects the amount of oligonucleotides adsorbed on the particle surface, thereby imparting stability to the particles. This finding has the potential to be generalized to other metal particle–oligonucleotide systems with borderline stability, helping to expand the repertoire of visible-range plasmon signatures useful for diagnostic application.

Introduction

The functionalization of Au nanoparticles with oligonucleotides *via* thiol–metal interaction, the aggregation of these conjugates induced by the hybridization of complementary DNA strands, and their applications in colorimetric DNA detection and diagnostics have been amply demonstrated,^{1–3} characterized,^{4–6} and modeled^{6,7} in various studies. Progress in this work and other such related works pertaining to DNA–nanoparticle systems has also been extensively reviewed in a recent article.⁸ Even more desirable for diagnostic applications might be to extend this capability of DNA–nanoparticle systems to multiplexing DNA detection, *e.g.*, employing a host of metal particles that can give a wide range of unique UV–visible plasmon signatures, thus providing greater flexibility, more rapid assay time, better reproducibility, and economy of sample and reagent use.⁹

Spherical silver nanoparticles—with a peak absorbance at ~380–400 nm, giving wide separation from that of gold’s 520 nm absorbance maximum, and equally straightforward preparation methods—are an ideal candidate for expanding the array of nanoparticles being employed for biomolecular detection. There has been an apparent difficulty in the functionalization of Ag particles with oligonucleotides *via* the well known thiol interaction with metals. Silver nanoparticle conjugates prepared by an analogous procedure used for Au were found to be unstable especially at the high ionic concentration required for subsequent hybridization. Only when they had been covered by a layer of Au in a core–shell structure were Ag particles functionalized in a sufficiently stable form fit for

hybridization conditions, while retaining their characteristic plasmon absorbance at the 380–400 nm wavelengths.¹⁰

This paper reports a successful preparation of the Ag–oligonucleotide conjugates by a simple modification of the analogous procedure for Au, without the need for an additional layer of Au coated on the Ag particles. The hybridization-induced aggregation of the conjugates is characterized by a UV–visible absorbance band shift, which can be used as a second “signature” distinct to that of Au or in combination with it. A sharp melting transition is also observed for this system, demonstrating its superior applicability to DNA melting-point determination.

Even more importantly, the dependence on pH as the critical factor for the stability of the prepared Ag conjugates is demonstrated. We explain this fact in terms of equilibrium adsorption of oligonucleotides on Ag nanoparticles, which is demonstrably pH-controlled, and discuss its implication to colloidal stability.

Experimental methods

Reagents and instrumentation

All oligonucleotides were purchased from Prologo. DTT (dithiothreitol) was purchased from Bio-Rad, and acetone purchased from Tedia. All salt solutions, including noble metal salts and phosphate buffers were prepared from reagent-grade stocks purchased from Merck. Water used was double-distilled, Milli-Q (18.2 MΩ).

All UV–visible absorbance spectra and kinetic measurements were obtained by Molecular Device Spectra-max 190 and Shimadzu UV-2450. Fluorescence measurements were recorded by BMG Labtechnologies Fluostar Optima. Melting point analyses were done on Amersham Biosciences Ultraspec® 3100 pro. Transmission Electron Microscope (a JEOL JEM2010 with acceleration voltage of 200 kV) was used to image and determine the sizes of Ag particles.

Metal nanoparticle preparation

Au nanoparticles of ~15 nm size were prepared by the well-known citrate method. Ag nanoparticles were prepared by the citrate-stabilized method as given by the literature,¹¹ using AgNO₃. Briefly: 1 mL of 0.01 M AgNO₃ was rapidly added to 99 mL of a solution of 0.30 mM Na citrate and 1 mM NaBH₄. This was done with vigorous stirring in an ice-cold bath. The solution rapidly changed to light yellow, after which stirring was continued up to 10 minutes. This method has been reported to yield Ag nanoparticles with a mean diameter of 10 nm.¹¹ Our own preparation yielded particles with an average diameter of 16 nm. Results of high-resolution transmission electron microscopy (HR-TEM), X-ray diffraction, and X-ray photoelectron spectroscopy (data not shown) all point to Ag(0) with no significant presence of either bulk or surface Ag oxide in the particles. The UV–visible spectrum of the resulting colloidal sol gave a sharp peak at 396 nm.

Metal nanoparticle functionalization

Ag nanoparticles were functionalized with complementary thiol-modified (5'-terminal thiol with C6 linker) oligonucleotides **1** and **2**, having sequence 5'-SH-C6-tta tat act taa aag caa ta-3' and 5'-SH-C6-ta ttg ctt tta agt ata taa-3', respectively. The complementary sequences were chosen to carry a majority of thymidine bases (shown to have the least affinity for Au surface) to lessen the non-specific binding to the metal surface, while minimizing self-hybridization and formation of secondary structures other than B-DNA duplex. Functionalization was carried out in several steps according to published procedures:¹² thiol-modified oligonucleotides were reacted with DTT (30 min at 37 °C) to ensure the complete reduction of disulfides. The dissolved excess DTT was solvent-extracted with dry acetone, and the oligonucleotides precipitated by the addition of Na acetate. Purified oligonucleotides were redispersed in water, and 0.5 nmole aliquots were added to 600 µL of Ag sol (as prepared, ~0.8 nM, assuming complete reduction of AgNO₃ and a particle size of 16 nm), giving a total strand-to-particle ratio of ~1050 : 1. The pH was then adjusted from ~6 to ~5 by adding NaH₂PO₄ (pH 4.1) to a final concentration of 10 mM and allowed to react for 24 h. Stepwise addition of NaCl up to 0.1 M was then made over another 24 h "aging" period, typically a three-step addition of salt at 8 h intervals.

The same method was followed for functionalizing both Ag and Au particles with thiol-modified adenine homo-oligonucleotide or SH-polyA and thymine homo-oligonucleotide or SH-polyT, both having 20-base length. For Au, 0.5 nmol of oligonucleotides was added to 200 µL sol (as prepared, ~8 nM), and no pH adjustment step was required prior to the stepwise addition of NaCl.

The solution pH was finally adjusted to pH 7 by the addition of Na phosphate buffer up to 20 mM just prior to ultracentrifuge separation (15 000 rpm for 15 min). The settled particles were dispersed in buffer containing 0.1 M NaCl and 10 mM Na phosphate (pH 7), to be referred here as 0.1 M PBS, and then made to undergo one more separation step to wash out oligonucleotides that were non-specifically bound, before finally dispersed in 0.3 M PBS buffer. The functionalized Ag particles gave an absorbance peak centered at 400 nm

(*vide infra*); this 4 nm shift from that of bare Ag particles is analogous to the observed shift for Au from 518 nm to 523 nm after DNA-modification.⁵

Hybridization-induced aggregation and UV–visible absorbance characterization

Equal volumes of Ag-nanoparticles bearing **1** and **2**, suspended in 0.3 M PBS, were mixed and allowed to stand for some period with shaking. Solutions containing only Ag-conjugates of either **1** or **2**, adjusted to give a similar concentration as the hybridizing mixture, were also prepared. UV-visible absorbance spectra were obtained for these preparations both right after mixing (~5 min with homogenization) and at specified time intervals up until 3 hours.

Melting-point demonstration of aggregated Ag nanoparticles

Following the same procedure and concentrations as in the preceding paragraph, complementary Ag-nanoparticle conjugates of **1** and **2**, and solutions containing non-complementary conjugates, were allowed to hybridize for 3 h at 37 °C, followed by annealing to room temperature, to ensure only perfect-match hybridization. The absorbance was monitored at the 400 nm wavelength, while the temperature was ramped from 40 °C to 70 °C at a rate of 2 °C min⁻¹.

Measurement of Ag particle aggregation with time in the presence of unmodified oligonucleotides

Ag-nanoparticle sol (20 µL as prepared, diluted to a final volume of 120 µL) containing unmodified polyA (0.04 nmoles), with and without pH modification (addition of NaH₂PO₄ [pH 4.1] to a final pH of 5), were added with NaCl, and their aggregation with time was followed by monitoring the attenuation of absorbance at 395 nm. Measurements were made in a multi-plate scanning mode to ensure simultaneous readings over a 20 min period, with scans made at 5 min intervals. Salt addition was done in two steps, at time 0 and 10 min, bringing the total concentration to 50 mM and 100 mM consecutively. Absorbance attenuation is reported as fraction remaining of the initial absorbance value obtained before the first salt addition.

Measurement of oligonucleotide equilibrium adsorption on Ag nanoparticles

Fluorescence-labelled (FAM) polyA (20-base length) were added to Ag nanoparticles to measure their equilibrium adsorption at different total strand-to-particle ratios, covering up to around 2500 : 1. Specifically, 0.005 nmol, 0.01 nmol, 0.02 nmol, and 0.04 nmol of FAM-polyA were each added to 6×-diluted Ag sols to a total volume of 120 µL in polypropylene microfuge tubes. The solutions were adjusted to pH 5 and pH 6 by the addition of appropriate phosphate buffers—NaH₂PO₄ (pH 4.1) and 4 : 7 Na₂HPO₄ : NaH₂PO₄ (pH 6), respectively—to a final 10 mM concentration. Wherever necessary, ionic strength of the solutions was varied by the addition of NaCl to 20 mM and 40 mM concentrations. The solutions were then allowed to stand for three hours at room temperature with continuous gentle shaking to ensure homogeneous mixing; after which, the solutions were centrifuged for 20 minutes at 13 200 rpm. The supernatant was then removed and transferred into a multi-well plate, where they were readjusted to pH 7 by the addition of PBS buffer (0.1 M final concentration) and read in the fluorospectrophotometer. The concentration of the adsorbed FAM-polyA was obtained by subtracting the measured FAM-polyA concentration in the supernatant from the known concentration added to the mixture, and expressed in terms of strands per Ag nanoparticle.

Results and discussion

The preparation of metal particle–oligonucleotide conjugates is a process of reacting the oligonucleotide's terminal thiol with the nanoparticles, followed by a gradual increase in salt concentration of the reaction solution. The increase should be gradual enough not to cause particle aggregation, since only charge repulsion is initially keeping the particles in colloidal suspension. Although the mechanism of the process has not been worked out in detail, the addition of salt is presumably to overcome the nucleotide–metal interactions, so that more of the adsorption sites on the particle surface become available to the terminal thiols. Thus, it may be assumed that in any prevailing condition, both thiols and nucleotides compete for adsorption sites, with the equilibrium shifting to favour thiol adsorption over nucleotide adsorption as the salt concentration increases. Finally, it may be possible to completely eliminate nucleotide adsorption after being 'crowded out' (steric hindrance) as more thiols adsorb to the metal.

While the above procedure has been shown useful for Au, it apparently is insufficient for producing silver nanoparticle–oligonucleotide conjugates. The addition of salt into the reaction solution (*i.e.*, nanoparticles plus the oligonucleotides) at the same increments used for Au would cause the Ag nanoparticles to aggregate irreversibly. The stability of the colloidal suspension in the presence of oligonucleotides, is a determining factor for this success (or failure) because of the difference in metal-affinity among the various nucleotides.¹³ For instance, we have observed that Ag nanoparticles with SH-polyA (adenine homo-oligonucleotide with thiol modification) were able to withstand the salt regimen, albeit producing a broader peak in the resulting absorbance spectrum indicative of slight aggregation, whereas SH-polyT (thymine homo-oligonucleotide with thiol modification) instantly aggregated on first-step salt addition (40 mM final concentration). Indeed, it has been shown that adenine has a greater affinity for Au than has thymine.¹³ Our observation points to the fact that success of this procedure depends on a critical balance between two requirements: colloidal stabilization by the oligonucleotides (which greatly depends on the nucleotide interactions with the metal) and the thiol interaction ultimately prevailing in the product conjugate (which depends on nucleotide interactions being diminished).

One of the ways to overcome the limitation imposed by the stability of Ag nanoparticles is coating the Ag nanoparticle with a thin layer of Au, producing a core–shell structure that retains the spectrophotometric signature of the silver core.¹⁰ This effective and convenient way of sidestepping the issue of stability may not be easily extended to other metals, depending on the ease with which a core–shell structure is obtained. Our present attempt is to demonstrate the potential of controlling charge concentrations of the interacting macromolecules as a way to sufficiently stabilize them for the conjugation reaction to proceed. By reducing the solution pH from 6 to 5 at the beginning of the reaction step, we were able to follow the same protocol that has been used for Au in functionalizing Ag nanoparticles with oligonucleotides.

Fig. 1 shows that the conjugates we have produced can selectively be aggregated in the presence of complementary oligonucleotides. The change in absorbance with time, monitored at the 400 nm wavelength absorbance maximum, for the complementary conjugates **1** and **2** in 0.3 M PBS is shown in Fig. 1A. Whereas the absorbance of the solution containing only conjugate **2** remained relatively stable throughout the 3 h monitoring period, the complementary conjugates declined in absorbance by more than 66%. The full absorbance spectra of the hybridized and non-hybridized conjugates, obtained after three hours in 0.3 M PBS, are shown in Fig. 1B. The aggregation of the conjugate pair **1** and **2** due to DNA hybridization, and their partial precipitation from the suspension, produced

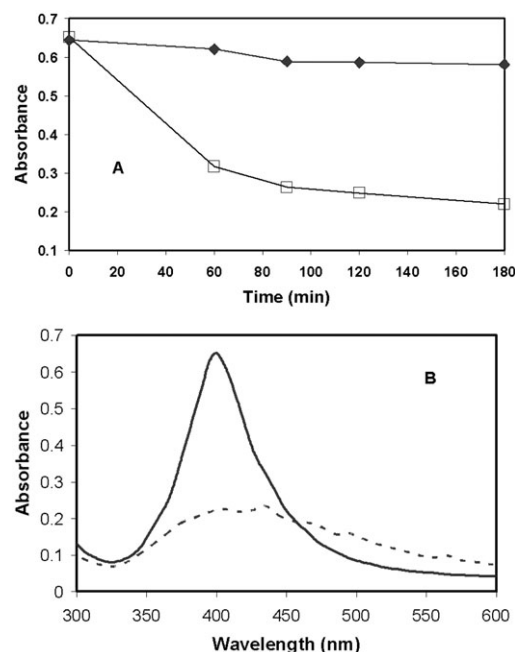


Fig. 1 A: Change with time in the 400 nm wavelength absorbance of conjugate **2** only (◆) and of complementary conjugate pair **1** and **2** (□). Whereas unpaired conjugate **2** showed minimal decrease in absorbance likely due to minor aggregation, the complementary conjugate pair showed a reduction in absorbance by 66% after 3 h in 0.3 M PBS, as a result of hybridisation-induced aggregation. B: Full absorbance spectra of the Ag–oligonucleotide conjugates, after 3 h in hybridizing condition of 0.3 M PBS: (–) complementary conjugates **1** and **2**; (—) conjugate **2** only.

the broadening and lowering of the original peak at 400 nm. No interparticle excitons were observed in the Ag–Ag particle aggregates.

As proof of the reversibility of the aggregation, the melting curve for the hybridized conjugates **1** and **2**, monitored at the 400 nm wavelength absorbance, is shown in Fig. 2. Comparisons of the melting endpoint with the original absorbance of the un-hybridized conjugates indicate a reversion of up to 77–89% of the original. Some degree of irreversibility can also be seen in Fig. 1A, wherein the absorbance of the non-hybridizing conjugate pairs stabilized at 90% the initial absorbance after about 3 h. A sharp melting transition (within 3–4 Celsius degrees) is observed, which contrasts with the melting curve of the native (*i.e.*, non-thiol modified, non-conjugated) oligonucleotides **1** and **2** that exhibits a broad transition (>10 Celsius degrees) as monitored at the 260 nm wavelength

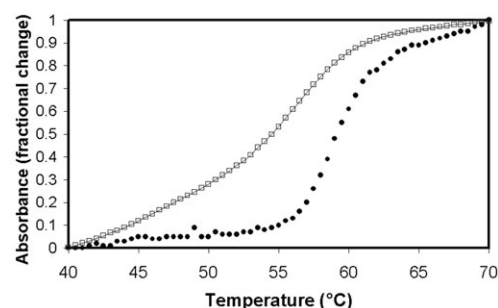


Fig. 2 Melting curve of aggregated conjugates **1** and **2** (shown as solid symbols), monitored at 400 nm wavelength absorbance, over the temperature range 40–70 °C (ramping at 2 °C min^{−1}). The transition occurs sharply within a 3–4 °C range, and slightly shifted from the melting point of the unmodified DNA (~55 °C). The melting curve of the unmodified DNA (shown as connected open symbols), monitored at 260 nm wavelength absorbance, shows a broad melting range spanning over 10 °C, in sharp contrast to the conjugate pair **1** and **2**.

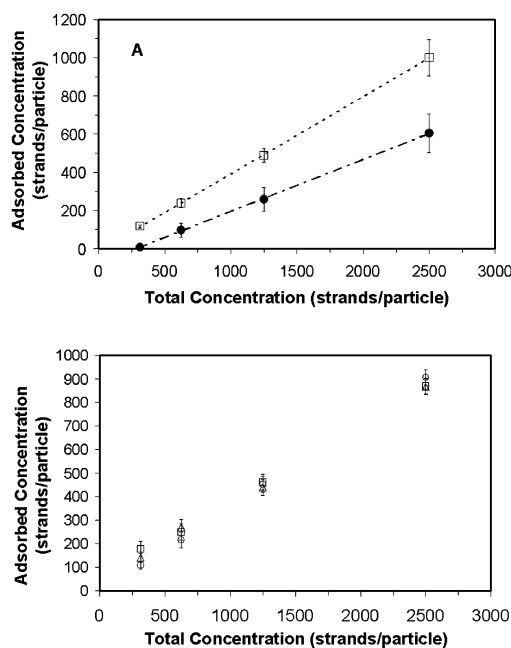


Fig. 3 A: PolyA adsorption on Ag nanoparticles expressed as strands adsorbed per particle. Panel A shows results for equilibrated solutions buffered at (□) pH 5 and (●) pH 6. B: Results for pH 5 buffered solutions having different ionic strengths: (○) without NaCl added; (△) 20 mM NaCl; (□) 40 mM NaCl. Adjusting the pH enhanced adsorption, while adjusting ionic strength had negligible effect.

absorbance (also shown in Fig. 2). This characteristic behaviour in metal–oligonucleotide conjugates has been attributed to an increased cooperativity of the melting process due to the multi-linkage network that holds together the nanoconjugate aggregates,⁷ making it an attractive candidate device for detecting mismatches that differ in melting points by only a few degrees. Note that there is a slight shift to a higher melting temperature in the conjugates from the native DNA's melting point ($\sim 55^\circ\text{C}$), another behaviour observed in this system owing to a stabilizing effect of the particle aggregate's coupled dielectric on the DNA duplex. No similar melting transition was observed when “bare” nanoparticles are aggregated in the presence of native (thus, non-specifically bound) oligonucleotides by the addition of high salt concentration, discounting the possibility of non-conjugated DNAs producing the observed melting transition in the hybridized conjugates.

To further examine how pH can affect the stability of the Ag nanoparticle–oligonucleotide system, we measured the equilibrium adsorption of oligonucleotides (in this experiment, FAM-polyA or FAM modified adenine homo-oligonucleotide) on the particles at the two different pH values of 6 and 5. Fig. 3A shows adsorbed concentrations (strands per particle) at different values of total concentration (summing both adsorbed strands and strands free in solution). The linear trend observed extends well into the highest concentration used, *i.e.*, 2500 strands per particle, which is already two-fold higher than what is used in the protocol.[†] The trends clearly reflect a significant enhancement in oligonucleotide adsorption as the pH is lowered from 6 to 5, with the difference monotonously increasing as total oligonucleotide concentration increases. At a total concentration of 1250 strands per particle (close to the concentration used in the functionalization procedure), the adsorbed concentration is 259 strands per particle (equivalent to $3.2 \times 10^{13} \text{ cm}^{-2}$), which then increases to nearly twice that

value after pH is lowered from 6 to 5. These high concentration values may in fact indicate additional layers of adsorbed oligonucleotides beyond the monolayer, which may be seen as further contributing to nanoparticle stabilization. Fig. 3B shows the equilibrium adsorption values at pH 5 with the addition of NaCl to 20 mM and 40 mM concentrations. The trend strongly suggests that the ionic strength does not influence oligonucleotide adsorption within the limit of the moderate concentrations used. Above around 50 mM NaCl, nanoparticle aggregation was already visible at low oligonucleotide concentrations. The increased adsorption observed in Fig. 3A is therefore the result of pH alone and not some artifact of the slight increase in the ionic strength due to buffer addition.

We hypothesize that the lower pH value causes the oligonucleotide to assume a less stretched out conformation, thereby allowing it to “pack” more closely together on the surface because of lesser inter-strand charge repulsion. This would require that the oligonucleotide displaces the weakly adsorbed citrate ions from the nanoparticle surface. This it can easily do, because apart from the nucleoside affinity for the metal, there is a cooperative binding enhancement from its polymeric nature.¹⁴ An alternative scenario suggested by Sandstrom *et al.* in 2003,¹⁵ involving dipole interactions, is unlikely, since it predicted increased adsorption by ion-shielding, which we did not observe when increasing ionic strength (*cf.* Fig. 3B).

To verify whether indeed an increase in oligonucleotide adsorption translates to greater stability of the Ag nanoparticles, we have subjected nanoparticles that are stabilized with unmodified polyA (adenine homo-oligonucleotide without modification), both adjusted to pH 5 and at pH 6, to increasing salt concentrations, and their absorbance at 395 nm wavelength (absorbance maximum of the “bare” Ag nanoparticles) monitored with time. Fig. 4 shows the results, along with nanoparticles not added with polyA as reference. The trend strongly suggests that buffering at pH 5 confers greater stability on the Ag nanoparticles stabilized with oligonucleotides, especially on initial addition of salt to 50 mM. Without pH adjustment, oligonucleotide-stabilized particles do not do significantly better than the reference. Further addition of salt to 100 mM reduced this ability of pH to influence stability, although oligonucleotide-stabilized nanoparticles continue to resist aggregation better than the reference. This is consistent with our earlier observation that salt concentration exerts little influence on oligonucleotide adsorption at the moderate concentration range of less than around 50 mM (Fig. 3B), leaving pH alone to determine stability from salt-induced particle aggregation, especially in this moderate salt-concentration range typically encountered early in the conjugate-formation process.

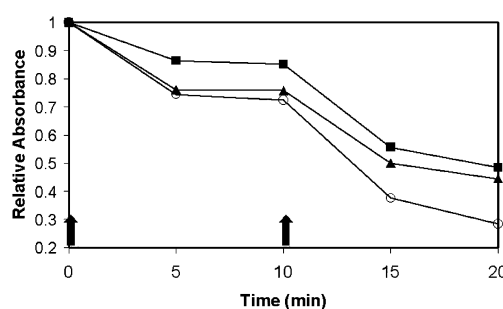


Fig. 4 Electrolyte-induced aggregation of Ag nanoparticles without polyA (○), and with polyA: (▲) unbuffered solution (pH ~ 6); (■) buffered at pH 5. Aggregation with respect to time is followed by monitoring the absorbance at 395 nm and expressed as a fraction of the initial, unperturbed absorbance. Two-step addition of NaCl—to 50 mM and 100 mM NaCl final concentrations—is indicated by broad arrows along the time axis.

[†] Extending this further would likely lead to saturation, but the expected errors at these high concentrations would become unacceptable since the data are generated by taking the difference of two large concentration values.

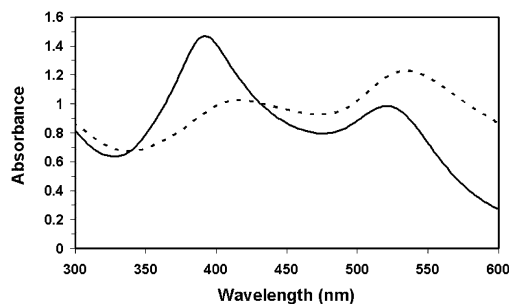


Fig. 5 UV-visible absorbance spectra of bimetallic conjugate mixtures containing polyA-Ag and polyT-Au conjugates (---), and Ag and Au conjugates both carrying polyA (—), in 0.3 M PBS (30 min hybridization). The shift in the absorbance band observed for the former exhibits an optical signature distinct from either metal's individual absorbance band shift.

Conclusions

We demonstrate in this paper the formation of stable conjugates of Ag nanoparticles and oligonucleotides that are capable of aggregating reversibly by DNA hybridization. We have shown that the key to stable conjugate formation is the control of pH during the functionalization process. Lowering the pH allows more oligonucleotides to adsorb on the nanoparticle surface, thus imparting stability to the nanoparticles from irreversible aggregation. This is especially the case in the early critical stage of the functionalization process, when the particle-oligonucleotide system is first challenged with moderate salt concentrations that are too low to significantly influence oligonucleotide adsorption, but high enough to induce particle aggregation.

Because the means for stabilizing the nanoparticles involves only the adjustment of the solution condition during the functionalization step, this approach should be fairly extendable to other systems, *i.e.*, to colloidal metal nanoparticles of borderline stability. Also, this straightforward approach has the potential to access other applications of nanoparticle-conjugates that may require a more specific surface material, which could not be attained simply by coating with Au.

Lastly, Fig. 5 illustrates a potential complementary use of this conjugate material in the well known diagnostics application of Au-oligonucleotide conjugates. Shown is the absor-

bance spectrum change when hybridizing Ag-PolyA conjugates with Au-PolyT. As in the Ag-Ag aggregates, no interparticle plasmon excitons were observed in the Ag-Au particle aggregates. This composite optical signature is characteristically distinct from that of the individual metal's response when hybridized separately (*i.e.*, Au with Au and Ag with Ag), thus potentially providing a three-way signal capability to a binary metal system.

Acknowledgements

This work is part of Singapore's Agency for Science, Technology and Research (A*Star) project #022-101-0038. We are grateful to Tai Du and Nivetha for the helpful discussions.

References

- 1 C. A. Mirkin, R. L. Letsinger, R. C. Mucic and J. J. Storhoff, *Nature*, 1996, **382**, 607-609.
- 2 A. P. Alivisatos, K. P. Johnsson, X. Peng, T. E. Wilson, C. J. Loweth, M. P. Bruchez Jr. and P. G. Schultz, *Nature*, 1996, **382**, 609-611.
- 3 J. J. Storhoff, R. Elghanian, R. C. Mucic, C. A. Mirkin and R. L. Letsinger, *J. Am. Chem. Soc.*, 1998, **120**, 1959-1964.
- 4 M. L. Sauthier, R. L. Carroll, B. G. Christopher and S. Franzen, *Langmuir*, 2002, **18**, 1825-1830.
- 5 S. R. Nicewarner-Pena, S. Raina, G. P. Goodrich, N. V. Fedoroff and C. D. Keating, *J. Am. Chem. Soc.*, 2002, **124**, 7314-7323.
- 6 J. J. Storhoff, A. A. Lazarides, R. C. Mucic, C. A. Mirkin, R. L. Letsinger and G. C. Schatz, *J. Am. Chem. Soc.*, 2000, **122**, 4640-4650.
- 7 R. Jin, G. Wu, Z. Li, C. A. Mirkin and G. C. Schatz, *J. Am. Chem. Soc.*, 2003, **125**, 1643-1654.
- 8 E. Katz and I. Willner, *Angew. Chem., Int. Ed.*, 2004, **43**, 6042.
- 9 S. G. Penn, L. He and M. J. Natan, *Curr. Opin. Chem. Biol.*, 2003, **7**, 609-615.
- 10 Y. W. Cao, R. Jin and C. A. Mirkin, *J. Am. Chem. Soc.*, 2001, **123**, 7961-7962.
- 11 T. Ung, L. M. Liz-Marzan and P. Mulvaney, *Langmuir*, 1998, **14**, 3740-3748.
- 12 L. M. Demers, C. A. Mirkin, R. C. Mucic, R. A. Reynolds III, R. L. Letsinger, R. Elghanian and G. Viswanadham, *Anal. Chem.*, 2000, **72**, 5535-5541.
- 13 J. J. Storhoff, R. Elghanian, C. A. Mirkin and R. L. Letsinger, *Langmuir*, 2002, **18**, 6666-6670.
- 14 M. M. Santore, in *Colloid Polymer Interactions*, ed. R. S. Farinato and P. L. Dubin, Wiley-Interscience, New York, 1999, Ch. 5.
- 15 P. Sandstrom, M. Boncheva and B. Akerman, *Langmuir*, 2003, **19**, 7537-7543.